



Structural Connectivity of Brain Regions May Predict Human Intelligence

Elahe Parham*, Mohamad Feshki*, Alireza Fallahi** and Hamid Soltanian-Zadeh*.,****.,***** (C.A.)

Abstract: The discovery of relationships between brain connectivity and human intelligence is of great interest. In this study, we identify structural connections correlated with human intelligence and investigate the predictability of intelligence from brain structural connectivity. The study uses data from 137 healthy subjects from the Human Connectome Project (HCP, 1200 Subjects Release). Structural connectivity was estimated using tractography derived from diffusion tensor imaging (DTI) data. A connectivity matrix was constructed using the mean fractional anisotropy (FA) of white-matter pathways between 116 regions defined by the AAL atlas. Global graph measures and correlation analysis were applied to identify connections relevant to predicting fluid intelligence (Gf) and crystallized intelligence (Gc). For prediction, three regression models of linear regression, support vector regression (SVR), and multi-layer perceptron (MLP) were employed. Most connections associated with Gf or Gc were located in the right hemisphere. Connections originating from prefrontal, right temporal, limbic, and right occipital regions were related to Gf, whereas connections originating from prefrontal, temporal, and left parietal regions were related to Gc. Among the models, SVR showed superior performance, achieving R^2 values of 0.45 and 0.52 for Gf and Gc, respectively. No significant relationships were observed between global graph measures and Gf or Gc scores. These findings demonstrate that DTI-based structural connectivity can be used to predict both fluid and crystallized intelligence, with fine-grained regional definitions enabling more specific connectivity patterns than in previous studies.

Keywords: Structural Connectivity, Brain Connectivity, Diffusion Tensor Imaging (DTI), Intelligence, Prediction.

1 Introduction

INTELLIGENCE can be defined as the capability of an individual to do purposeful performance, logical

thinking, and effective interaction with the environment [1]. The emergence of intelligence tests in psychometrics allows the measurement and quantification of mental abilities. These tests may be used to study the relationship between mental capabilities and behavioral, environmental, and genetic factors. One of the most well-known tests is WAIS-III, which is used for individuals above 16 years old [2]. Another one is the NIH toolbox [3]. The result of each test is an assessment of one of the cognitive capabilities of an individual. Because cognitive impairment is often associated with neurological disorders such as autism spectrum disorder (ASD), intelligence tests are a powerful tool for clinical screening [4]. Initial attempts utilized positron emission tomography (PET) to study the neural substrates of intelligence [5], [6]. In a few years, magnetic resonance imaging (MRI) took over PET for the study of the brain's macroscopic structure and its relationship with

Iranian Journal of Electrical & Electronic Engineering, 2026.

Paper first received 07 Jun 2025 and accepted 30 Jan 2026.

* The authors are with the School of Electrical and Computer Engineering, Faculty of Engineering, University of Tehran, Tehran, Iran.

** The author is with the Biomedical Engineering Department, Hamedan University of Technology, Hamedan, Iran.

*** The author is with the Medical Image Analysis Lab, Departments of Radiology and Research Administration, Henry Ford Health System, Detroit, MI, USA.

**** The author is with the School of Cognitive Sciences, Institute for Research in Fundamental Sciences (IPM), Tehran, Iran

Corresponding Author: Hamid Soltanian-Zadeh.

E-mails: hsoltan1@hfhs.org, hszadeh@ut.ac.ir

intelligence [7], [8]. Based on the results achieved by MRI studies, several theories were proposed about the neural basis of human intelligence, including the Lateral Prefrontal Cortex Theory (LPFCT) [9], the Parieto-Frontal Integration theory (P-FIT) [10], [11], [12], [13], the Multiple-Demand theory (M-DT) [14] and Process Overlap theory (POT) [15]. These theories collectively emphasize the critical role of distributed and interacting brain regions—particularly frontal and parietal areas—in supporting higher cognitive. While these models were initially derived from functional activation or morphometric evidence, they implicitly rely on the existence of efficient structural pathways that enable information exchange between regions participating in reasoning, problem solving, and knowledge retrieval.

Previous neuroimaging studies have primarily explored the functional or gray-matter correlates of intelligence [16], [17]. However, functional connectivity reflects dynamic, state-dependent synchronization, and morphometric indices describe localized structure without revealing how information physically travels between regions. In contrast, structural connectivity, as measured by diffusion tensor imaging (DTI), provides a stable representation of the brain's anatomical wiring, which underlies both transient functional interactions and long-term cognitive learning. Examining white-matter connections therefore offers unique insight into how information-processing efficiency contributes to individual differences in intelligence [18], [19], [20], [21], [22].

Within this framework, fractional anisotropy (FA) serves as a theoretically and practically justified feature: it reflects microstructural properties such as axonal density, organization, and myelination, which influence the speed and reliability of signal transmission. Higher FA values indicate more coherent and efficient white-matter fibers—biological properties that directly relate to information integration efficiency. Therefore, FA is particularly well-suited for modeling fluid intelligence (Gf), which depends on rapid and flexible processing across distributed networks, and crystallized intelligence (Gc), which relies on the stability of knowledge-related connections between temporal and parietal regions.

Recent studies have reported significant relationships between and intelligence in multiple tracts, including right inferior fronto-occipital fasciculus [23], callosum splenium [24], [25], [26], and tracts between the medial orbital frontal cortex and rostral anterior cingulate cortex [27]. These findings suggest that higher FA, reflecting better myelination and fiber organization, may facilitate more efficient neural communication and thus higher cognitive performance.

Building upon this theoretical and empirical foundation, the present study investigates how whole-

brain structural connectivity—quantified as mean FA of white-matter pathways between 116 regions defined by the Automated Anatomical Labeling (AAL) atlas—relates to individual differences in fluid (Gf) and crystallized (Gc) intelligence. In addition to regional connections, we examined the associations between global network characteristics and intelligence using several graph-theoretical measures. The strength of this study lies in its comprehensive and fine-grained approach: each ROI represents a small, anatomically defined brain region, enabling detailed mapping of structural pathways across the entire brain. To assess the predictive value of these features, we applied three regression models—Support Vector Regression (SVR), Multilayer Perceptron (MLP), and Linear Regression (LR)—allowing direct comparison of model performance.

Based on this framework, we addressed two main research questions: (1) Can individual differences in Gf and Gc be predicted from whole-brain structural connectivity patterns derived from DTI? (2) Which specific white-matter connections and global graph measures contribute most strongly to these predictions? We hypothesized that higher FA, reflecting greater white-matter integrity and inter-regional communication efficiency, would be associated with higher Gf and Gc. Specifically, Gf was expected to show stronger associations with fronto-parietal and cingulo-opercular pathways supporting cognitive control and flexible reasoning, whereas Gc was expected to involve temporal and parietal connections linked to language and semantic knowledge. Furthermore, we anticipated that models based on fine-grained regional connectivity would outperform those using global network measures in explaining individual variability in intelligence

2 Materials and Methods

2.1 Participants

We used publicly available data from the Human Connectome Project (HCP, 1200 Subjects Release), which includes high-quality, standardized diffusion-weighted imaging (DWI) and cognitive measures across a large cohort of healthy adults [28]. The dataset's uniform acquisition protocols and preprocessing pipelines ensure reproducibility and comparability across subjects. The dataset consists of 137 subjects (70 male and 67 female), mean age of 28.43 years. All participants completed the NIH toolbox cognitive function battery (CFB) [28], [29]. All these subjects were healthy, without any brain damage. In addition, none of them had a history of mental illness, brain surgery, or brain-damaging disease.

2.2 Image Acquisition

The subjects of the HCP dataset were scanned using a spin-echo EPI DTI sequence with the following

parameters: repetition time = 5520 ms, echo time = 89.5 ms, flip angle = 78 degrees, field of view = 210×180 mm, slice thickness = 1.25 mm (111 slices), and b-values of 1000, 2000, and 3000 s/mm².

2.3 Cognitive Tasks

The Gf score was calculated by averaging the scores of five cognitive tasks which measure short-term memory [30], long-term memory [31], processing speed [32], and two executive functions [33] determined using the NIH toolbox. The Gc score was the average of two cognitive tasks including vocabulary comprehension and reading decoding [34]. The mean (standard deviation) of the Gf and Gc scores were 106.20 (±13.26) and 102.18 (±8.93), respectively.

2.4 DTI Image Processing

The HCP DWI images were processed using the diffusion pipeline of FSL's EDDY (v3.19.0), which improved slice outlier detection and removed the noise caused by the subject movement. Then, the registration were performed using ExploreDTI v4.8.6, which provides improved motion correction and spatial normalization pipelines compatible with the HCP data format. For tractography and structural connectivity matrix construction, we used ExploreDTI v4.6.8, as this version offers stable and reproducible results for large-scale deterministic tractography using the AAL atlas. The use of two versions was intentional, to combine the enhanced registration accuracy of v4.8.6 with the proven tractography stability of v4.6.8.

2.5 DTI Fiber Tracking

For each subject, using Explore-DTI (v4.6.8), DTI-based tractography was done for the whole brain by a deterministic approach based on streamlined algorithms where the local tract direction was defined by the major eigenvector of the diffusion tensor. This was done for a fiber length range of 10-500 mm, angle threshold of 30 degrees, and FA range of [0.2-1]. The connectivity matrix (116×116) was obtained between the nodes of the AAL atlas template, using Explore-DTI (v4.6.8). In the connectivity matrix, each element is the average value of FA in the connections between two regions. Each edge's FA weight was calculated by averaging the FA values of all the fibers that comprised the edge. The FA value of each fiber was determined by taking the average of the FA values of all the voxels in the fiber track. In our calculations, if a tract between two nodes extended to another node, that node was considered the terminator of the pathway. For example, if region A was connected to region B and region B was connected to region C, then, C was considered as the terminator, i.e., region A was considered to be connected to region C. We performed 1,000,000 streamlined tracking iterations, with each iteration having a unique sample of the parameter combination

2.6 Global Graph Measure Analysis

To examine the relation of brain global structural characteristics with Gf and Gc scores, we computed the following global graph measures: characteristic path length, global efficiency, and global clustering coefficient. The characteristic path length of a network is defined as the average shortest path length between all pairs of nodes in the network. On the other hand, the global efficiency of a network is defined as the inverse of the shortest path length. Unlike the characteristic path length, global efficiency can be meaningfully computed on disconnected networks, making it a superior measure of integration [35], [36]. The global clustering coefficient is a measure of functional integration and reflects, on average, the prevalence of clustered connectivity around individual nodes [36]. To obtain binary connectivity matrices, we applied a proportional thresholding method to remove the weakest connections generated by tractography. Because the choice of threshold strongly influences network topology and density, it must be carefully determined. In this study, a proportional threshold of 0.25 was selected, retaining the top 25% of the strongest connections to balance network sparsity and completeness. This level minimizes false-positive connections arising from tractography noise while preserving the core structural organization of the brain network, consistent with prior DTI-based graph studies [37], [38].

2.7 Feature Selection and Reduction

To perform statistical analysis, we first applied correlation analysis between the mean FA value of each connection, age, and sex of the subjects and the Gf and Gc scores using MATLAB (R2017a) to identify the variables highly correlated with the Gf and Gc scores.

Model performance was evaluated using leave-one-out cross-validation (LOOCV), which trains the model on all participants except one and tests on the held-out subject in each iteration. LOOCV was chosen because it maximizes data usage in moderate-sized samples and provides nearly unbiased estimates of model generalization, as commonly applied in neuroimaging-based predictive modeling studies (Scheinost et al., 2019; Shen et al., 2017). Although alternative strategies such as k-fold cross-validation or external validation can further test generalizability, the current sample size and data availability limited this approach.

First, we removed the connections that had zero variance. Second, we removed the connections whose linear regression with the Gf and Gc scores was not significant (p-value < 0.05). Finally, we removed the feature that had high correlations to another feature (r > 0.95) and retained the feature that had a higher correlation with the intelligence score. The feature selection process was carried out solely on the training

set, and during testing, only the selected features were computed and utilized. Principal Component Analysis (PCA) was applied to reduce feature dimensionality by retaining components that together explained 85% of the total variance in the structural connectivity features. This threshold was selected empirically to balance variance preservation and model simplicity, consistent with prior studies using DTI or functional connectivity features for intelligence prediction [39], [40].

2.8 Regression Models

Three regression models including linear regression; support vector regression (SVR); and multilayer perceptron (MLP) were applied to the data to predict the Gf and Gc scores. Then, we calculated R2, correlation, and RMSE between the predicted and measured intelligence scores to identify the model with the best performance.

3 Results

Correlations of Gc and Gf scores with age and sex The Gf and Gc scores were calculated for 137 subjects (112.23 ± 7.52 and 115.50 ± 8.84 , respectively). Correlation analysis was performed between age/sex and the Gf/Gc scores. The results are shown in Table 1, indicating that correlation analysis does not reveal any significant relationships between Gf and age and sex, using the Benjamini-Hochberg adjusted p-value to consider multiple comparisons. This is consistent with previous studies that found no sex differences between fluid intelligence and crystal intelligence [41], [42], [43].

To compare the results of significant relationships between Gf/Gc and age/sex parameters with previous studies, we applied ANOVA [44]. This test was used to check whether there were significant differences between the means of Gf and Gc of males and females. We found that there were no statistically significant differences between the two groups for Gf (p-value = 0.08) and Gc (p-value = 0.95). Besides, we calculated the effect size (Cohen's d (Cohen, 1988)) to quantify the difference between the two means. We found small effect sizes ($d < 0.5$) for both Gc and Gf. The results, presented in Table 1, show the consistency of our results with those of previous studies.

To compare the two brain hemispheres, we performed a correlation analysis on the connections in the right and left hemispheres. The connections that had a significant relationship with Gf or Gc are shown in Fig. 1 (a, b).

In the right hemisphere, there are 25 and 29 connections that are significantly correlated with Gf and Gc, respectively, and in the left hemisphere, there are 11 and 25 connections. A greater proportion of predictive connections were observed in the right hemisphere,

suggesting a predominant involvement of right-hemisphere networks in intelligence-related structural organization.[45], [46], [47], [48], [49].

Table 1. Correlations of Gc and Gf with age and, correlations, ANOVA, and effect size of Gc and Gf with sex of the subjects and the corresponding p-values, adjusted using Benjamini-Hochberg procedure.

Variables	Correlation	p-value	F (df)	d
Gf - age	-0.09	0.34	-	-
Gc - age	0.19	0.08	-	-
Gf - sex	0.17	0.08	0.01 (1)	0.01
Gc - sex	-0.004	0.95	5.39 (1)	0.39
Gf [41]	-	-	0.00 (1.56)	0.00
Gc [41]	-	-	0.28 (1.56)	0.00
Culture-Fair Test (Gf) [43]	-	-	-	0.10
Progressive matrices (Gf) [43]	-	-	-	0.02
Vocabulary (Gc) [42]	-	-	0.28 (1)	-
Synonyms (Gc) [42]	-	-	0.27 (1)	-
Antonyms (Gc) [42]	-	-	1.08 (1)	-

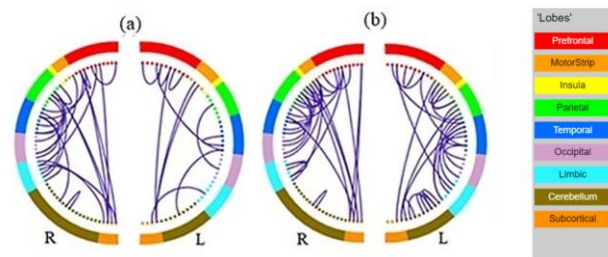


Fig 1. Intra-hemispheric connections that have significant correlations with: (a) Gf, and (b) Gc.

3.1 Correlation of global graph measures with Gc and Gf scores

The results of examining the relation between characteristic path length, global efficiency, and global clustering coefficient were demonstrated in Table 2. These results show there is no significant relationship between the global graph measures and the Gc and Gf scores.

Table 2. Performance of three models developed for the relation of Gf and Gc global graph parameters.

Intelligence Score	Model	Characteristic path length		Global efficiency		Global clustering coefficient	
		r	p-value	r	p-value	r	p-value
Linear regression	Gf	0.14	0.11	0.08	0.37	0.08	0.34
	SVR	0.14	0.11	0.08	0.37	0.08	0.34
	MLP	0.00	1.00	0.00	1.00	0.14	0.11
Linear regression	Gc	0.07	0.42	0.09	0.29	0.01	0.90
	SVR	-0.07	0.42	0.09	0.29	-0.01	0.90
	MLP	0.07	0.42	-0.14	0.11	0.07	0.42

3.2 Correlation of Selected Features with Gc and Gf Scores

The connectivity matrix, calculated for the 137 subjects, is symmetric and the elements show average FA in the connections between the corresponding regions. To predict the Gf and Gc scores, we had $(116 \times 116 - 116) / 2 = 6670$ distinct connections for each subject. Fig 2 shows the most frequent connections among all training sets before PCA analysis which shows the best features for predicting Gf and Gc scores. Based on the leave-one-out cross-validation algorithm the number of selected features was different in each training set and the mean value of the test sets were reported. The parameters of the models were varied and then the resulting models were tested. The Pearson correlation coefficient between the measured and predicted scores for Gf and Gc using linear regression were $r = 0.71$ (p-value = 2.82×10^{-15}) and $r = 0.66$ (p-value = 9.81×10^{-13}), respectively.

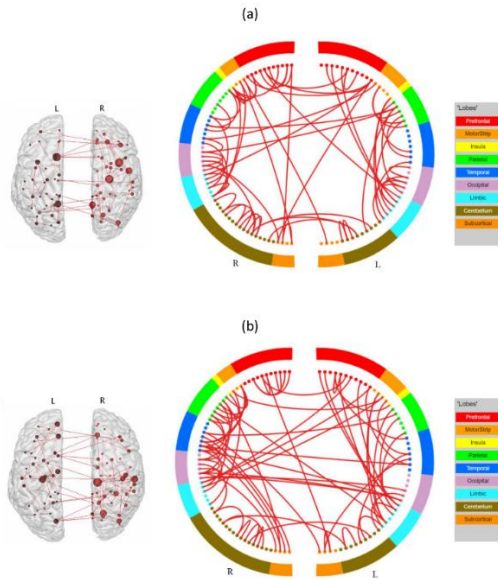


Fig 2. The most frequent connections (intra- and inter-hemispheric) selected for developing prediction models for: (a) Gf, and (b) Gc scores.

The SVR model was evaluated using both linear and radial basis function (RBF) as a kernel. The linear kernel was evaluated with constant parameters 1, 10, 50, and 100. The best performance was obtained when the constant parameter was 10, where for the Gf and Gc scores, the correlations were $r = 0.72$ (p-value = 6.84×10^{-17}) and $r = 0.68$ (p-value = 9.93×10^{-13}). The RBF kernel was evaluated using constant parameters 50 and 100 and gamma values of 0.1, 0.01, and 0.001. To predict Gf, the highest correlation was obtained using SVR and RBF kernel function (constant = 50 and gamma = 0.1), which was $r = 0.68$ (p-value = 2.65×10^{-15}). To predict Gc, using the same model with constant

= 100 and gamma = 0.1, the highest correlation was $r = 0.65$ (p-value = 1.09×10^{-11}).

The MLP model was developed with one layer using different neurons and an identity layer. The best performance was achieved for predicting Gf using 3 neurons ($r = 0.65$, p-value = 1.49×10^{-9}) and for predicting Gc using 17 neurons ($r = 0.63$, p-value = 1.39×10^{-10}).

The optimal performance of each model is shown in Table 3 and the regression lines with 95% confidence intervals are plotted in Figure 3. The results illustrate that the correlation values are higher when predicting Gc than Gf. Besides, the root mean square error (RMSE) is lower when predicting Gf than Gc. This suggests that Gf is more predictable from structural connectivity than Gc.

Table 3. Optimal performance of three models developed for predicting Gf and Gc from structural connectivity of the brain regions. The results of the superior method are highlighted.

Model	Intelligence Score	R ²	r	p-value	RMS E
Linear regression	Gf	0.50	0.71	2.82E-15	7.31
SVR	Gf	0.51	0.72	6.84E-17	7.11
MLP	Gf	0.42	0.65	1.42E-09	8.07
Linear regression	Gc	0.43	0.66	9.81E-13	11.34
SVR	Gc	0.46	0.68	9.93E-13	11.26
MLP	Gc	0.39	0.63	1.39E-10	11.66

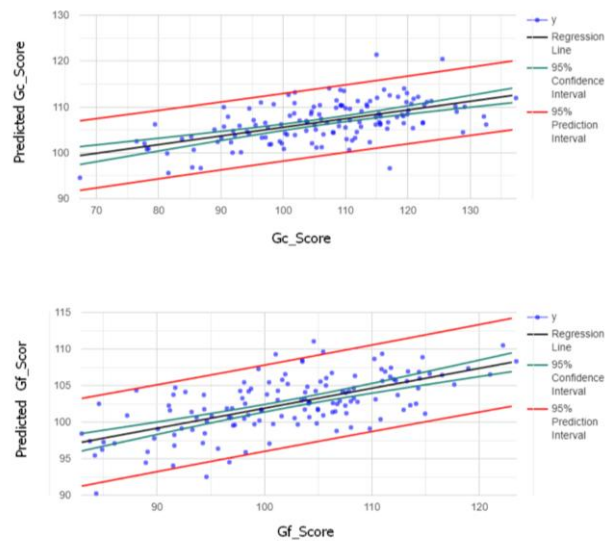


Fig 3. Optimal regression lines with 95% confidence intervals for predicting Gf and Gc from the structural connectivity matrix.

The results show that the SVR model with a linear kernel and a constant parameter of 10 is the optimal model for predicting both Gf and Gc. The results of this work are compared with those of the previous models in Table 4. Note that the model proposed for predicting intelligence has a higher determination coefficient in comparison with the previous methods. Moreover, previous methods have widely used functional MRI data to predict intelligence. In contrast, we have used DTI data and mean FA of connections to predict intelligence.

Table 4. Results of the previous methods of predicting human intelligence from the structural and functional features of the brain.

Study	Intelligence	Imaging	Model	Brain region(s)	R ²
Choi (2008)	General intelligence	Anatomical and functional MRI	Linear regression	Whole cortex	0.44
Wang (2015)	General intelligence	Anatomical MRI	Multi-kernel SVR	Volume of gray matter and white matter	0.52
Wang (2015)	General intelligence	Anatomical MRI	Single-kernel SVR	Volume of gray matter and white matter	0.46
Finn (2015)	Fluid intelligence	Functional MRI	CPM	Whole brain	0.06
Finn (2015)	Fluid intelligence	Functional MRI	CPM	Fronto-parital network	0.25
Dubois (2018)	Fluid intelligence	Functional MRI	Univariate correlation filtering + Elastic net regression	Gray matter	0.04
Dubois (2018)	General intelligence	Functional MRI	Univariate correlation filtering + Elastic net regression	Whole cortex	0.20
Present study	Fluid intelligence	DWI	Linear kernel SVR	Whole brain	0.52
Present study	Crystalized intelligence	DWI	Linear kernel SVR	Whole brain	0.45

To study the reason for scattering in the estimated intelligence scores, we defined two homogeneous subgroups with high intelligence (HI) and low intelligence (LI) scores, respectively. Each group consisted of 50 subjects based on their Gf (LI: 92.07 ± 8.16 and HI: 119.39 ± 5.85) or Gc (LI: 92.67 ± 4.70 and HI: 111.31 ± 4.35) scores. The overlaps between low Gc and low Gf groups, high Gc and high Gf groups, low Gc and high Gf groups, and high Gc and low Gf groups were 50%, 40%, 32%, and 20%, respectively.

The connections correlated with Gf or Gc scores in both groups were identified, and the connections significantly related to Gf and Gc in each group are shown in Figure S1 (Supplementary Materials). The high-degree nodes identified in each group are presented in Figure S2. For Gf, connections highly correlated with high scores originated mainly from prefrontal, temporal, limbic, and cerebellar regions, whereas for Gc they originated from prefrontal, parietal, and subcortical regions.

Next, we defined two homogeneous subgroups based on the connectivity matrices. Each group consisted of 50 subjects (Table S1, Supplementary Materials). A one-way ANOVA test revealed no significant differences between the Gf and Gc scores of these subgroups. Figure S3 and Figure S4 show the identified connections and high-degree nodes for each group. For Gc, although the selected connections differed, similar regional patterns were observed among high-degree nodes. For Gf, one subgroup exhibited more high-degree nodes in the limbic region, whereas the other showed more in the prefrontal region

4 Discussion

The present study contributes to the growing field of intelligence neuroscience by introducing a methodologically integrated framework that combines DTI-based structural connectivity, fine-grained brain parcellation, and machine learning-based prediction. Unlike previous investigations that primarily relied on regional morphometric indices (e.g., cortical volume or thickness) or resting-state functional connectivity, our approach uses whole-brain tractography-derived connectivity matrices constructed from the AAL-116 atlas, capturing detailed inter-regional interactions across the entire white-matter network. Moreover, by implementing both support vector regression (SVR) and multilayer perceptron (MLP) models, we were able to assess both linear and nonlinear relationships between structural connectivity features and intelligence measures. This integrative strategy provides a comprehensive, fine-grained, and data-driven perspective on how structural brain networks support fluid and crystallized intelligence, representing a clear advancement beyond previous modality-specific studies.

Our findings suggest that the effects of age and sex are negligible or small when studying Gf and Gc. Previous work studying Gc and Gf [41], [42] showed that there were no significant differences in the overall performance between men and women. However, to be on the safe side, one may control for age and sex in the analysis.

Interestingly, none of the global graph measures showed significant correlations with fluid or crystallized intelligence. This finding suggests that overall

topological efficiency or global network integration may not be the primary determinants of individual differences in intelligence. Instead, intelligence may depend more strongly on specific regional or inter-regional connections, particularly those within the fronto-parietal and temporo-limbic networks that support executive and integrative cognitive processes. This interpretation aligns with previous findings indicating that local efficiency and subnetwork-level organization, rather than global connectivity, better capture the neural substrates of cognitive performance [50], [51]. In this context, the absence of a global relationship reinforces the view that intelligence emerges from specialized yet interactively coordinated neural circuits, rather than from uniform whole-brain integration.

The observed predominance of right-hemisphere and prefrontal connectivity in predicting intelligence is consistent with previous neuroimaging studies linking right-lateralized fronto-parietal networks to reasoning, cognitive control, and abstract problem-solving [45], [52], [53]. Our findings therefore confirm and extend these earlier results by demonstrating that similar patterns emerge when modeling *structural connectivity* rather than functional activation or gray-matter volume. Furthermore, the identified contributions of temporal and limbic pathways to crystallized intelligence align with prior reports emphasizing the role of semantic memory and emotional regulation networks in knowledge-based abilities [46], [47], [48], [49]. Taken together, these findings reinforce the view that intelligence arises from the efficient integration of distributed—but functionally specialized—white-matter systems supporting executive, associative, and semantic processes.

Beyond the predominant involvement of prefrontal and parietal regions, our analyses also revealed contributions from limbic and occipital areas, particularly in relation to fluid intelligence (Gf). The limbic network—including regions such as the cingulate and hippocampus—may support emotional regulation, motivation, and adaptive behavior, all of which facilitate flexible reasoning and problem-solving. This interpretation aligns with evidence that emotional and motivational processes influence executive functioning and cognitive control [54], [55]. The involvement of occipital regions likely reflects their role in visuospatial integration and perceptual organization, cognitive processes that are fundamental to abstract reasoning and pattern recognition tasks that typically load on Gf. In contrast, the temporal and inferior parietal regions associated with crystallized intelligence (Gc) are consistent with networks supporting semantic memory, language comprehension, and knowledge retrieval, which contribute to accumulated verbal and experiential knowledge [12], [56]. Together, these findings suggest

that intelligence depends not only on executive and associative hubs but also on the dynamic integration of perceptual, emotional, and semantic systems.

The subjects were divided into high and low-intelligence groups to study the differences between the two groups. A related study showed that the number of tracts in the brain's structural network is significantly larger in the group with high intelligence scores than in the group with low intelligence scores [57]. Here, we assessed how the number of connections related to the differences in the two groups. Differences of the structural connections in the brain between the groups of high and low Gf and Gc were studied to identify the connections that can explain the difference of the intelligence scores. The literature revealed that intelligence was related to the structure and function of the temporal, hippocampal [58], and prefrontal [59] regions. Our results showed that the prefrontal, right temporal, and occipital regions were influential since the connections correlated with Gf and Gc mostly originated from these regions. In addition, connections originating from the limbic region were correlated with Gc.

Predictably human intelligence was evaluated in the past using the brain's morphological parameters [60], [61] or functional connectivity measures [62]. Regional cortical thickness had strong explanatory importance and explained over 30% of the variance in intelligence ($R^2 = 0.302$). This parameter had better performance than local surface area, sulcal depth, or absolute mean curvature [61]. Moreover, resting-state functional connectivity matrices explained about 20% of the inter-subject variability of general intelligence [62]. The intelligence could be predicted using cortical and subcortical gray matter parameters ($R^2 = 0.044$) and ROIs in the whole brain cortex ($R^2 = 0.206$). Multi-kernel SVR model was used to study the predictability of intelligence ($R^2 = 0.516$, $r = 0.71$) using cerebral gray and white matter regional volume [60] which had the best performance among the previous studies summarized in Table 3.

The correlations of 0.72 and 0.68 were obtained for Gf and Gc, respectively, indicating a good association. Comparing RMSE for the prediction of Gf and Gc, it was shown that the RMSEs of the models predicting Gf were less than those of models predicting Gc. A comparison of RMSE shows that Gf is more predictable than Gc.

We used a structural connectivity matrix to train the models. In comparison with functional connectivity and morphometric parameters, structural connectivity measures led to smaller errors. In addition, the SVR approach was the most suitable model for predicting human intelligence from the connectivity of brain regions.

These findings indicate that the structural connectivity patterns underlying intelligence are highly individualized. Rather than reflecting a single, uniform network organization, intelligence appears to emerge from multiple alternative structural configurations. Individuals with similar intelligence levels may rely on different sets of white-matter connections, while similar connectivity patterns can coincide with varying cognitive performance. This variability suggests that intelligence estimation based on limited connection subsets may be suboptimal, and incorporating additional parameters—such as regional efficiency, network modularity, or multimodal features—may improve predictive accuracy.

One methodological limitation concerns the use of leave-one-out cross-validation (LOOCV) as the sole validation strategy. While LOOCV provides a nearly unbiased estimate of model performance in smaller datasets, it may still be susceptible to overfitting when the number of features is high relative to the sample size. Future research should address this by incorporating independent test sets or multi-site validation cohorts, which would enhance the robustness and generalizability of the predictive models.

Another methodological consideration concerns the tractography procedure used to construct the connectivity matrices. Streamlines were counted between regions even if they passed through a third ROI, which may reduce anatomical specificity by allowing indirect pathways to contribute to connectivity strength. However, this choice was intentional to retain sensitivity to long-range, integrative white-matter tracts that facilitate communication between distributed cortical systems—networks known to support higher-order cognitive processes such as reasoning and problem-solving. Because identical tractography parameters were applied across all subjects, any potential inflation in streamline counts was systematic and unlikely to bias between-subject comparisons or predictive modeling results.

5 Conclusion

The goal of this study was to assess the predictability of human intelligence from structural connectivity of the brain regions, estimated from the DTI data. Correlation analysis showed negligible effects of age and sex on Gf and Gc. However, there were significant differences in the average FA of the brain connections. The majority of the connections correlated with Gf and Gc were in the right hemisphere. The differences in the structural connections of the brains of the high and low Gf and Gc groups were studied. The results showed that the prefrontal, temporal, and occipital regions were most relevant since the connections highly correlated with Gf and Gc originated from these regions. In addition,

connections originating from the limbic regions were correlated with Gf. Using leave-one-out cross-validation, SVR with a linear kernel and a constant parameter of 10 was the best regression model to predict Gf and Gc scores.

Conflict of Interest

The authors declare no conflict of interest.

Author Contributions

Conceptualization and supervision: Hamid Soltanian-Zadeh; Methodology, investigation, and writing – original draft: Elahe Parham and Mohamad Feshki; Data analysis and manuscript editing: Alireza Fallahi; Writing – review & editing: All authors; Funding acquisition and resources: Hamid Soltanian-Zadeh.

Funding

This work was supported in part by the Cognitive Sciences and Technologies Council of Iran under the Iran-Brazil Collaboration Desk.

Informed Consent Statement

Informed consent was not necessary because publicly available, deidentified data with IRB approval was used.

Acknowledgment

Data were provided by the Human Connectome Project, WU-Minn Consortium (Principal Investigators: David Van Essen and Kamil Ugurbil; 1U54MH091657) funded by the 16 NIH Institutes and Centers that support the NIH Blueprint for Neuroscience Research; and by the McDonnell Center for Systems Neuroscience at Washington University.

References

- [1] D. Wechsler, *The measurement of adult intelligence (3rd ed.)*. Baltimore: Williams & Wilkins Co, 1946. doi: 10.1037/11329-000.
- [2] R. Westerhausen *et al.*, “The corpus callosum as anatomical marker of intelligence? A critical examination in a large-scale developmental study,” *Brain Struct. Funct.*, vol. 223, no. 1, pp. 285–296, Jan. 2018, doi: 10.1007/s00429-017-1493-0.
- [3] S. Weintraub *et al.*, “I. NIH TOOLBOX COGNITION BATTERY (CB): INTRODUCTION AND PEDIATRIC DATA,” *Monogr. Soc. Res. Child Dev.*, vol. 78, no. 4, pp. 1–15, Aug. 2013, doi: 10.1111/mono.12031.
- [4] T. Charman, A. Pickles, E. Simonoff, S. Chandler, T. Loucas, and G. Baird, “IQ in children with autism spectrum disorders: data from the Special Needs and Autism Project (SNAP),” *Psychol. Med.*, vol. 41, no. 3, pp. 619–627, Mar. 2011, doi: 10.1017/S0033291710000991.
- [5] T. N. Chase, “Wechsler Adult Intelligence Scale

- Performance,” *Arch. Neurol.*, vol. 41, no. 12, p. 1244, Dec. 1984, doi: 10.1001/archneur.1984.04050230026012.
- [6] R. J. Haier *et al.*, “Cortical glucose metabolic rate correlates of abstract reasoning and attention studied with positron emission tomography,” *Intelligence*, vol. 12, no. 2, pp. 199–217, Apr. 1988, doi: 10.1016/0160-2896(88)90016-5.
- [7] J. K. Kroger, “Recruitment of Anterior Dorsolateral Prefrontal Cortex in Human Reasoning: a Parametric Study of Relational Complexity,” *Cereb. Cortex*, vol. 12, no. 5, pp. 477–485, May 2002, doi: 10.1093/cercor/12.5.477.
- [8] V. Prabhakaran, J. A. L. Smith, J. E. Desmond, G. H. Glover, and J. D. E. Gabrieli, “Neural Substrates of Fluid Reasoning: An fMRI Study of Neocortical Activation during Performance of the Raven’s Progressive Matrices Test,” *Cogn. Psychol.*, vol. 33, no. 1, pp. 43–63, Jun. 1997, doi: 10.1006/cogp.1997.0659.
- [9] J. Duncan and A. M. Owen, “Common regions of the human frontal lobe recruited by diverse cognitive demands,” *Trends Neurosci.*, vol. 23, no. 10, pp. 475–483, Oct. 2000, doi: 10.1016/S0166-2236(00)01633-7.
- [10] M. W. Cole, T. Yarkoni, G. Repovs, A. Anticevic, and T. S. Braver, “Global Connectivity of Prefrontal Cortex Predicts Cognitive Control and Intelligence,” *J. Neurosci.*, vol. 32, no. 26, pp. 8988–8999, Jun. 2012, doi: 10.1523/JNEUROSCI.0536-12.2012.
- [11] M. W. Cole, T. Ito, and T. S. Braver, “Lateral Prefrontal Cortex Contributes to Fluid Intelligence Through Multinetwork Connectivity,” *Brain Connect.*, vol. 5, no. 8, pp. 497–504, Oct. 2015, doi: 10.1089/brain.2015.0357.
- [12] R. E. Jung and R. J. Haier, “The Parieto-Frontal Integration Theory (P-FIT) of intelligence: Converging neuroimaging evidence,” *Behav. Brain Sci.*, vol. 30, no. 2, pp. 135–154, Apr. 2007, doi: 10.1017/S0140525X07001185.
- [13] M. Song *et al.*, “Brain spontaneous functional connectivity and intelligence,” *Neuroimage*, vol. 41, no. 3, pp. 1168–1176, Jul. 2008, doi: 10.1016/j.neuroimage.2008.02.036.
- [14] J. Duncan, “The multiple-demand (MD) system of the primate brain: mental programs for intelligent behaviour,” *Trends Cogn. Sci.*, vol. 14, no. 4, pp. 172–179, Apr. 2010, doi: 10.1016/j.tics.2010.01.004.
- [15] K. Kovacs and A. R. A. Conway, “Process Overlap Theory: A Unified Account of the General Factor of Intelligence,” *Psychol. Inq.*, vol. 27, no. 3, pp. 151–177, Jul. 2016, doi: 10.1080/1047840X.2016.1153946.
- [16] E. A. de Souza, S. A. Silva, B. H. Vieira, and C. E. G. Salmon, “fMRI functional connectivity is a better predictor of general intelligence than cortical morphometric features and ICA parcellation order affects predictive performance,” *Intelligence*, vol. 97, p. 101727, Mar. 2023, doi: 10.1016/j.intell.2023.101727.
- [17] B. H. Vieira, G. S. P. Pamplona, K. Fachinello, A. K. Silva, M. P. Foss, and C. E. G. Salmon, “On the prediction of human intelligence from neuroimaging: A systematic review of methods and reporting,” *Intelligence*, vol. 93, p. 101654, Jul. 2022, doi: 10.1016/j.intell.2022.101654.
- [18] D. J. Madden *et al.*, “Influence of structural and functional brain connectivity on age-related differences in fluid cognition,” *Neurobiol. Aging*, vol. 96, pp. 205–222, Dec. 2020, doi: 10.1016/j.neurobiolaging.2020.09.010.
- [19] Y. N. Kenett *et al.*, “Driving the brain towards creativity and intelligence: A network control theory analysis,” *Neuropsychologia*, vol. 118, pp. 79–90, Sep. 2018, doi: 10.1016/j.neuropsychologia.2018.01.001.
- [20] T. Ohtani *et al.*, “Exploring the neural substrates of attentional control and human intelligence: Diffusion tensor imaging of prefrontal white matter tractography in healthy cognition,” *Neuroscience*, vol. 341, pp. 52–60, Jan. 2017, doi: 10.1016/j.neuroscience.2016.11.002.
- [21] E. Parham, M. Feshki, and H. Soltanian-Zadeh, “Relation between Brain Structural Connectivity and Processing Speed,” in *2018 25th National and 3rd International Iranian Conference on Biomedical Engineering (ICBME)*, IEEE, Nov. 2018, pp. 1–5, doi: 10.1109/ICBME.2018.8703583.
- [22] D. A. Pisner, R. Smith, A. Alkozei, A. Klimova, and W. D. S. Killgore, “Highways of the emotional intellect: white matter microstructural correlates of an ability-based measure of emotional intelligence,” *Soc. Neurosci.*, vol. 12, no. 3, pp. 253–267, May 2017, doi: 10.1080/17470919.2016.1176600.
- [23] Y. Wang *et al.*, “Sex differences in white matter development during adolescence: A DTI study,” *Brain Res.*, vol. 1478, pp. 1–15, Oct. 2012, doi: 10.1016/j.brainres.2012.08.038.
- [24] J. D. Clayden *et al.*, “Normative Development of White Matter Tracts: Similarities and Differences in Relation to Age, Gender, and Intelligence,” *Cereb. Cortex*, vol. 22, no. 8, pp. 1738–1747, Aug. 2012, doi: 10.1093/cercor/bhr243.
- [25] B. Dunst, M. Benedek, K. Koschutnig, E. Jauk, and A. C. Neubauer, “Sex differences in the IQ-

- white matter microstructure relationship: A DTI study,” *Brain Cogn.*, vol. 91, pp. 71–78, Nov. 2014, doi: 10.1016/j.bandc.2014.08.006.
- [26] F. J. Navas-Sánchez *et al.*, “White matter microstructure correlates of mathematical giftedness and intelligence quotient,” *Hum. Brain Mapp.*, vol. 35, no. 6, pp. 2619–2631, Jun. 2014, doi: 10.1002/hbm.22355.
- [27] P. G. Nestor *et al.*, “Dissociating prefrontal circuitry in intelligence and memory: neuropsychological correlates of magnetic resonance and diffusion tensor imaging,” *Brain Imaging Behav.*, vol. 9, no. 4, pp. 839–847, Dec. 2015, doi: 10.1007/s11682-014-9344-6.
- [28] D. C. Van Essen, S. M. Smith, D. M. Barch, T. E. J. Behrens, E. Yacoub, and K. Ugurbil, “The WU-Minn Human Connectome Project: An overview,” *Neuroimage*, vol. 80, pp. 62–79, Oct. 2013, doi: 10.1016/j.neuroimage.2013.05.041.
- [29] N. Akshoomoff *et al.*, “VIII. NIH TOOLBOX COGNITION BATTERY (CB): COMPOSITE SCORES OF CRYSTALLIZED, FLUID, AND OVERALL COGNITION,” *Monogr. Soc. Res. Child Dev.*, vol. 78, no. 4, pp. 119–132, Aug. 2013, doi: 10.1111/mono.12038.
- [30] D. S. Tulsky *et al.*, “NIH Toolbox Cognition Battery (NIHTB-CB): List Sorting Test to Measure Working Memory,” *J. Int. Neuropsychol. Soc.*, vol. 20, no. 6, pp. 599–610, Jul. 2014, doi: 10.1017/S135561771400040X.
- [31] P. J. Bauer, S. S. Dikmen, R. K. Heaton, D. Mungas, J. Slotkin, and J. L. Beaumont, “III. NIH Toolbox Cognition Battery (CB): measuring episodic memory,” *Monogr. Soc. Res. Child Dev.*, vol. 78, no. 4, pp. 34–48, Aug. 2013, doi: 10.1111/mono.12033.
- [32] N. E. Carlozzi, D. S. Tulsky, R. V. Kail, and J. L. Beaumont, “VI. NIH TOOLBOX COGNITION BATTERY (CB): MEASURING PROCESSING SPEED,” *Monogr. Soc. Res. Child Dev.*, vol. 78, no. 4, pp. 88–102, Aug. 2013, doi: 10.1111/mono.12036.
- [33] P. D. Zelazo *et al.*, “NIH Toolbox Cognition Battery (CB): Validation of Executive Function Measures in Adults,” *J. Int. Neuropsychol. Soc.*, vol. 20, no. 6, pp. 620–629, Jul. 2014, doi: 10.1017/S1355617714000472.
- [34] R. C. Gershon *et al.*, “IV. NIH TOOLBOX COGNITION BATTERY (CB): MEASURING LANGUAGE (VOCABULARY COMPREHENSION AND READING DECODING),” *Monogr. Soc. Res. Child Dev.*, vol. 78, no. 4, pp. 49–69, Aug. 2013, doi: 10.1111/mono.12034.
- [35] S. Achard and E. Bullmore, “Efficiency and Cost of Economical Brain Functional Networks,” *PLoS Comput. Biol.*, vol. 3, no. 2, p. e17, Feb. 2007, doi: 10.1371/journal.pcbi.0030017.
- [36] M. Rubinov and O. Sporns, “Complex network measures of brain connectivity: Uses and interpretations,” *Neuroimage*, vol. 52, no. 3, pp. 1059–1069, Sep. 2010, doi: 10.1016/j.neuroimage.2009.10.003.
- [37] V. J. Schmithorst and S. K. Holland, “A comparison of three methods for generating group statistical inferences from independent component analysis of fMRI data,” *J. Magn. Reson. Imaging*, vol. 19, no. 3, pp. 365–368, 2004.
- [38] P. Kochunov *et al.*, “Processing speed is correlated with cerebral health markers in the frontal lobes as quantified by neuroimaging,” *Neuroimage*, vol. 49, no. 2, pp. 1190–1199, Jan. 2010, doi: 10.1016/j.neuroimage.2009.09.052.
- [39] D. Scheinost *et al.*, “Ten simple rules for predictive modeling of individual differences in neuroimaging,” *Neuroimage*, vol. 193, pp. 35–45, Jun. 2019, doi: 10.1016/j.neuroimage.2019.02.057.
- [40] D. A. Llano *et al.*, “A novel dynamic network imaging analysis method reveals aging-related fragmentation of cortical networks in mouse,” *Netw. Neurosci.*, vol. 5, no. 2, pp. 569–590, Jun. 2021, doi: 10.1162/netn_a_00191.
- [41] A. S. Kaufman, J. C. Kaufman, X. Liu, and C. K. Johnson, “How do Educational Attainment and Gender Relate to Fluid Intelligence, Crystallized Intelligence, and Academic Skills at Ages 22-90 Years?,” *Arch. Clin. Neuropsychol.*, vol. 24, no. 2, pp. 153–163, Mar. 2009, doi: 10.1093/arclin/acp015.
- [42] S. Muglia Wechsler *et al.*, “Gender differences on tests of crystallized intelligence,” *Eur. J. Educ. Psychol.*, vol. 7, no. 1, p. 59, Oct. 2015, doi: 10.30552/ejep.v7i1.98.
- [43] D. van der Linden, C. S. Dunkel, and G. Madison, “Sex differences in brain size and general intelligence (g),” *Intelligence*, vol. 63, pp. 78–88, Jul. 2017, doi: 10.1016/j.intell.2017.04.007.
- [44] Henry Scheffé, *The Analysis of Variance*. Wiley-Interscience, 1999.
- [45] A. K. Barbey, R. Colom, E. J. Paul, and J. Grafman, “Architecture of fluid intelligence and working memory revealed by lesion mapping,” *Brain Struct. Funct.*, vol. 219, no. 2, pp. 485–494, Mar. 2014, doi: 10.1007/s00429-013-0512-z.
- [46] M. Beeman, “Semantic Processing in the Right Hemisphere May Contribute to Drawing Inferences from Discourse,” *Brain Lang.*, vol.

- 44, no. 1, pp. 80–120, Jan. 1993, doi: 10.1006/brln.1993.1006.
- [47] R. Le Grand, C. J. Mondloch, D. Maurer, and H. P. Brent, “Expert face processing requires visual input to the right hemisphere during infancy,” *Nat. Neurosci.*, vol. 6, no. 10, pp. 1108–1112, Oct. 2003, doi: 10.1038/nn1121.
- [48] T. Horowitz-Kraus, Y. Wang, E. Plante, and S. K. Holland, “Involvement of the right hemisphere in reading comprehension: A DTI study,” *Brain Res.*, vol. 1582, pp. 34–44, Sep. 2014, doi: 10.1016/j.brainres.2014.05.034.
- [49] M. Vigneau *et al.*, “What is right-hemisphere contribution to phonological, lexico-semantic, and sentence processing?,” *Neuroimage*, vol. 54, no. 1, pp. 577–593, Jan. 2011, doi: 10.1016/j.neuroimage.2010.07.036.
- [50] J. D. Kruschwitz, L. Waller, L. S. Daedelow, H. Walter, and I. M. Veer, “General, crystallized and fluid intelligence are not associated with functional global network efficiency: A replication study with the human connectome project 1200 data set,” *Neuroimage*, vol. 171, pp. 323–331, May 2018, doi: 10.1016/j.neuroimage.2018.01.018.
- [51] K. Hilger, M. Ekman, C. J. Fiebach, and U. Basten, “Efficient hubs in the intelligent brain: Nodal efficiency of hub regions in the salience network is associated with general intelligence,” *Intelligence*, vol. 60, pp. 10–25, Jan. 2017, doi: 10.1016/j.intell.2016.11.001.
- [52] H. R. Colom R, Jung RE, “Distributed brain sites for the g-factor of intelligence,” *Neuroimage*, vol. 31, no. 3, 2006, doi: 10.1016/j.neuroimage.2006.01.006.
- [53] V. Ponsoda *et al.*, “Structural brain connectivity and cognitive ability differences: A multivariate distance matrix regression analysis,” *Hum. Brain Mapp.*, vol. 38, no. 2, pp. 803–816, Feb. 2017, doi: 10.1002/hbm.23419.
- [54] L. Pessoa, “On the relationship between emotion and cognition,” *Nat. Rev. Neurosci.*, vol. 9, no. 2, pp. 148–158, Feb. 2008, doi: 10.1038/nrn2317.
- [55] A. K. Barbey, R. Colom, and J. Grafman, “Distributed neural system for emotional intelligence revealed by lesion mapping,” *Soc. Cogn. Affect. Neurosci.*, vol. 9, no. 3, pp. 265–272, Mar. 2014, doi: 10.1093/scan/nss124.
- [56] J. R. Binder and R. H. Desai, “The neurobiology of semantic memory,” *Trends Cogn. Sci.*, vol. 15, no. 11, pp. 527–536, Nov. 2011, doi: 10.1016/j.tics.2011.10.001.
- [57] Y. Li *et al.*, “Brain Anatomical Network and Intelligence,” *PLoS Comput. Biol.*, vol. 5, no. 5, p. e1000395, May 2009, doi: 10.1371/journal.pcbi.1000395.
- [58] “Intelligence and brain structure in normal individuals,” *Am. J. Psychiatry*, vol. 150, no. 1, pp. 130–134, Jan. 1993, doi: 10.1176/ajp.150.1.130.
- [59] J. DUNCAN, “Frontal Lobe Function and General Intelligence: Why it Matters,” *Cortex*, vol. 41, no. 2, pp. 215–217, 2005, doi: 10.1016/S0010-9452(08)70896-7.
- [60] L. Wang, C.-Y. Wee, H.-I. Suk, X. Tang, and D. Shen, “MRI-Based Intelligence Quotient (IQ) Estimation with Sparse Learning,” *PLoS One*, vol. 10, no. 3, p. e0117295, Mar. 2015, doi: 10.1371/journal.pone.0117295.
- [61] J.-J. Yang *et al.*, “Prediction for human intelligence using morphometric characteristics of cortical surface: Partial least square analysis,” *Neuroscience*, vol. 246, pp. 351–361, Aug. 2013, doi: 10.1016/j.neuroscience.2013.04.051.
- [62] J. Dubois, P. Galdi, Y. Han, L. K. Paul, and R. Adolphs, “Resting-State Functional Brain Connectivity Best Predicts the Personality Dimension of Openness to Experience,” *Personal. Neurosci.*, vol. 1, p. e6, Jul. 2018, doi: 10.1017/pen.2018.8.

Biographies

Elahe Parham, is a researcher and research assistant at the CERVO Brain Research Centre, Faculty of Science and Engineering, Université Laval. She completed her PhD in Biophotonics at Université Laval in 2025. He received his M.Sc. degree in Electrical engineering from University of Tehran in 2018 and B.Sc Degree from Electrical engineering from Amirkabir University of Technology- Tehran Polytechnic in 2015. Her research involves optical methods, brain imaging and data analysis.

Mohamad Feshki, is a doctoral researcher and research assistant at the CERVO Brain Research Centre, Faculty of Science and Engineering, Université Laval. He is PhD student in Electrical Engineering at Université Laval. He received his M.Sc. degree in Biomedical Engineering from University of Tehran in 2019. His research involves artificial intelligence, computational imaging, medical imaging and biophotonics.



Alireza Fallahi, is Assistant Professor in Biomedical Engineering Department, Hamedan University of Technology, Hamedan, Iran. He received His Ph.D and M.Sc. degree in Biomedical Engineering from Shahed University in 2020 and 2010 respectively. He received His B.sc. degree in Electrical Engineering from Tabriz University in 2007. His research involves Medical Signal and Image Processing and Brian imaging and analysis.



Hamid Soltanian-Zadeh, is a full Professor and a founder of Control and Intelligent Processing Center of Excellence (CIPCE) in the Department of Electrical and Computer Engineering at the University of Tehran, Tehran, Iran. He received B.Sc and M.Sc degrees in electrical engineering: electronics (with honors) from the University of Tehran, Tehran, Iran in 1985 and 1987 respectively . He received PhD degrees in Electrical Engineering: systems and bio-electrical sciences from the University of Michigan, Ann Arbor, Michigan, USA, in 1992. His research involves Image Processing, Medical Imaging, Pattern Recognition and Neural Networks.